AFRL-ML-WP-TP-2007-513

OPTICAL TUNING OF THE REFLECTION OF AZOBENZENE LIQUID CRYSTAL DOPED CHOLESTERICS (PREPRINT)

Uladzimir A. Hrozhyk, Svetlana V. Serak, Nelson V. Tabiryan, and Timothy J. Bunning

Hardened Materials Branch
Survivability and Sensor Materials Division

APRIL 2007

AIR FORCE RESEARCH LABORATORY
MATERIALS AND MANUFACTURING DIRECTORATE
WRIGHT-PATTERSON AIR FORCE BASE, OH 45433-7750
AIR FORCE MATERIEL COMMAND
UNITED STATES AIR FORCE

NOTICE AND SIGNATURE PAGE

Using Government drawings, specifications, or other data included in this document for any purpose other than Government procurement does not in any way obligate the U.S. Government. The fact that the Government formulated or supplied the drawings, specifications, or other data does not license the holder or any other person or corporation; or convey any rights or permission to manufacture, use, or sell any patented invention that may relate to them.

This report was cleared for public release by the Air Force Research Laboratory Wright Site (AFRL/WS) Public Affairs Office and is available to the general public, including foreign nationals. Copies may be obtained from the Defense Technical Information Center (DTIC) (http://www.dtic.mil).

AFRL-ML-WP-TP-2007-513 HAS BEEN REVIEWED AND IS APPROVED FOR PUBLICATION IN ACCORDANCE WITH ASSIGNED DISTRIBUTION STATEMENT.

*//Signature//

TIMOTHY J. BUNNING, Ph.D.
Research Lead
Exploratory Development
Hardened Materials Branch

//Signature//

MARK S. FORTE, Acting Chief
Hardened Materials Branch
Survivability and Sensor Materials Division

//Signature//

TIM J. SCHUMACHER, Chief
Survivability and Sensor Materials Division

This report is published in the interest of scientific and technical information exchange, and its publication does not constitute the Government's approval or disapproval of its ideas or findings.

*Disseminated copies will show "//Signature//" stamped or typed above the signature blocks.

REPORT DOCUMENTATION PAGE

Form Approved
OMB No. 0704-0188

1. REPORT DATE *(DD-MM-YY)*	2. REPORT TYPE	3. DATES COVERED *(From - To)*
April 2007	Journal Article Preprint	

4. TITLE AND SUBTITLE
OPTICAL TUNING OF THE REFLECTION OF AZOBENZENE LIQUID CRYSTAL DOPED CHOLESTERICS (PREPRINT)

5a. CONTRACT NUMBER
In-house

5b. GRANT NUMBER

5c. PROGRAM ELEMENT NUMBER
62102F

6. AUTHOR(S)
Uladzimir A. Hrozhyk, Svetlana V. Serak, and Nelson V. Tabiryan (Beam Engineering for Advanced Measurements Corporation)
Timothy J. Bunning (AFRL/MLPJ)

5d. PROJECT NUMBER
4348

5e. TASK NUMBER
RG

5f. WORK UNIT NUMBER
M08R1000

7. PERFORMING ORGANIZATION NAME(S) AND ADDRESS(ES)

Beam Engineering for Advanced Measurements Corporation
809 South Orlando Ave., Suite I
Winter Park, FL 32789

Hardened Materials Branch (AFRL/MLPJ)
Survivability and Sensor Materials Division
Materials and Manufacturing Directorate
Wright-Patterson Air Force Base, OH 45433-7750
Air Force Materiel Command, United States Air Force

8. PERFORMING ORGANIZATION REPORT NUMBER
AFRL-ML-WP-TP-2007-513

9. SPONSORING/MONITORING AGENCY NAME(S) AND ADDRESS(ES)
Air Force Research Laboratory
Materials and Manufacturing Directorate
Wright-Patterson Air Force Base, OH 45433-7750
Air Force Materiel Command
United States Air Force

10. SPONSORING/MONITORING AGENCY ACRONYM(S)
AFRL/MLPJ

11. SPONSORING/MONITORING AGENCY REPORT NUMBER(S)
AFRL-ML-WP-TP-2007-513

12. DISTRIBUTION/AVAILABILITY STATEMENT
Approved for public release; distribution unlimited.

13. SUPPLEMENTARY NOTES
Journal article submitted to Advanced Functional Materials. The U.S. Government is joint author of this work and has the right to use, modify, reproduce, release, perform, display, or disclose the work.

PAO Case Number: AFRL/WS 07-0176, 29 Jan 2007.

14. ABSTRACT
Mixtures of cholesteric liquid crystals doped with high clearing temperature azobenzene nematic liquid crystals are shown to possess large, fast, and reversible dynamic photosensitive features. Selective wavelengths shifts approaching 400 nm are reported and depending on the host cholesteric liquid crystal, both red-shifted and blue-shifted wavelength changes can be induced. The photoinduced states of these material systems are shown to be stable for long periods of time upon removal of the radiation source, completely reversible, and dynamically fast. These phototunable features were demonstrated using both CW and nanosecond laser beams. The latter was used to change the selective reflection wavelength from blue to green with a single nanosecond pulse and the ability to write information into these films using these processes were demonstrated.

15. SUBJECT TERMS
Liquid Crystal (LC), Cholesteric Liquid Crystal (CLC), Azobenzene Nematic Liquid Crystal (azo NLC)

16. SECURITY CLASSIFICATION OF:			17. LIMITATION OF ABSTRACT:	18. NUMBER OF PAGES	19a. NAME OF RESPONSIBLE PERSON (Monitor)
a. REPORT	b. ABSTRACT	c. THIS PAGE			Timothy J. Bunning
Unclassified	Unclassified	Unclassified	SAR	46	19b. TELEPHONE NUMBER *(Include Area Code)* N/A

Standard Form 298 (Rev. 8-98)
Prescribed by ANSI Std. Z39-18

Optical Tuning of the Reflection of Azobenzene Liquid Crystal Doped Cholesterics**

By Uladzimir A. Hrozhyk, Svetlana V. Serak, Nelson V. Tabiryan and Timothy J. Bunning*

Mixtures of cholesteric liquid crystals doped with high clearing temperature azobenzene nematic liquid crystals are shown to possess large, fast, and reversible dynamic photosensitive features. Selective wavelengths shifts approaching 400 nm are reported and depending on the host cholesteric liquid crystal, both red-shifted and blue-shifted wavelength changes can be induced. The photoinduced states of these material systems are shown to be stable for long periods of time upon removal of the radiation source, completely reversible, and dynamically fast. These phototunable features were demonstrated using both CW and nanosecond laser beams. The latter was used to change the selective reflection wavelength from blue to green with a single nanosecond pulse and the ability to write information into these films using these processes were demonstrated.

---

[*] Dr. U. Hrozhyk, Dr. S. Serak, Dr. N. Tabiryan

Beam Engineering for Advanced Measurements Corporation

809 South Orlando Ave., Suite I, Winter Park, FL 32789 (USA)

Dr. T.J Bunning

Air Force Research Laboratory

Wright-Patterson Air Force Base, Ohio 45433-7707 (USA)

E-mail: timothy.bunning@wpafb.af.mil; 937-255-9649; 937-255-1128

[**] This work was supported by an AFOSR/SBIR/STTR Program and AFOSR/NL

Table of Contents Text and Graphic

Cholesteric liquid crystals doped with high clearing temperature azobenzene liquid crystals are shown to possess large (>400 nm), fast, and reversible dynamic selective wavelengths. These photosensitive features were demonstrated using both CW and nanosecond laser beams.

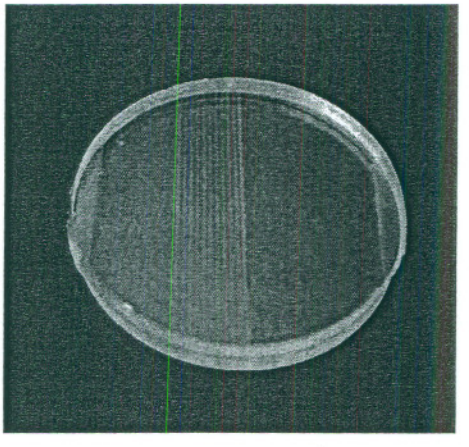

1. Introduction

Photonics technologies, including optical communications, image processing, and adaptive optics require efficient means for controlling the propagation of optical radiation. Liquid crystal (LC) electro-optical devices are at the core of many current photonic applications including beam-steerers, displays, switches, and dynamic gratings. Large changes in the refractive index, low power requirements and a robust manufacturing base have driven this commercial success. Cholesteric liquid crystals (CLC's) may combine the large optical anisotropy typical for nematic LC's with a 1-dimensional photonic band gap structure. When aligned into the so-called planar texture, this periodic structure results from a macroscopic rotation of the director caused by molecular chirality. Such structures are distinguished by Bragg reflection of circularly polarized light beam of the same handedness of the CLC,[1] and when a wavelength commensurate with the visible portion of the spectrum is present, bright reflective color is observed. Both the width $\Delta\lambda$ and the position λ_B of the CLC reflection band are determined by the pitch h of the CLC, $\Delta\lambda = h(n_{||} - n_{\perp})$ and $\lambda_B = hn$, where $n_{||}$ and $n_{\perp}$ are the local principal values of the refractive indices of the CLC and $n = (n_{||} + n_{\perp})/2$ is the average refractive index.

The ability to modulate the Bragg reflection color, both position and strength, has been a practical goal which has driven numerous previous research efforts. The periodic helical structure of a CLC can be controlled with external influences, including electrical fields, temperature and optical radiation thus enabling dynamic Bragg gratings. The electro-optical behavior of CLC's has been explored with a number of different materials

including both positive and negative dielectric materials and is discussed in numerous publications.[2] Most of this work has centered on enabling fast, binary switching (on-off) of the reflection notch. However, because of the rather slow relaxation of electrically-induced structural changes in CLC's and the formation of strongly light scattering focal conic textures in that process, optical systems based on nematic and smectic LC's are more prevalent in display and variable color filter applications due to their higher speed of operation and simpler electro-optical characteristics.[3-4]

The ability to dynamically change the color (wavelength tuning) has also been investigated. Complex electrode geometries, negative dielectric systems, and polymer-stabilized CLC's have shown limited success in enabling large wavelength tuning. More recently, the ability to use the radiation itself as the actuating mechanism in a variety of non-cholesteric LC-based systems has been investigated by incorporating various light-responsive chromophores into the LC materials.[5-8] Reversible light-induced changes in molecular conformation of a photochromic guest molecule is typically used to affect local LC-ordering. The ability to use this process to effectively (and reversibly) modulate the pitch of a CLC and consequently the Bragg reflection wavelength over a wide range has been a long sought goal although numerous papers discussing exposure to radiation have been published before[9-20] with the first observation dated as far back as to 1971.[10] Typical shifts of the reflection notch wavelength observed to date using UV radiation were 100-150 nm.

We report here on the development of phototunable CLCs based on azobenzene nematic LCs (azo NLCs) with extraordinarily large optical nonlinearity and photosensitivity. The development of azo-based LC molecules which possess large

mesogenic temperature ranges spanning room temperature[21] allows for a large concentration to be mixed with doped into commercially available CLC's. This enables large color tuning via irradiation of microwatt and even nanowatt power light beams due to photoisomerization processes of the azobenzene core. Due to a wide mesophase temperature region range and a high clearing temperature, the subsequent trans-cis isomerization of these dopants in the host CLC affects both the molecular order and the 'effective' helical twisting power of the mixture without thrusting the mixture through the typical isothermal phase transition. We demonstrate here phototunable (stable and reversible) Bragg reflective materials that shift their peak wavelength ~ 400 nm due to UV radiation, the highest shift reported to date. Materials that exhibit both blue and red shifts relative to the original selective wavelength using low power UV radiation are demonstrated. Once irradiated, the materials are stable for long periods of times (hours) and the reverse wavelength shift can be induced with green and red laser wavelengths. In a dramatic demonstration, a material that has had its original green selective wavelength shifted to the blue via UV irradiation is shown to respond to single nanosecond pulses of a green laser beam. These pulses induce a 'reverse' red shift of the reflective notch back to the green and patterns can be easily written using scanned beams. These CLC materials demonstrate the possibility of wide area thin films that autonomously respond to radiation of a given wavelength enabling new generation all-optical material systems.

2. Results and Discussion

Figure 1a shows the typical absorption spectrum of azo NLC 1205 (BEAM Co.) in NLC 5CB (Merck). Figure 1b shows the Bragg reflection wavelength vs azo dopant concentration for a mixture of CLC 1445 (Merck) and azo NLC's 1005 (BEAM Co.). [21] Note that namely azo NLCs are considered as dopant in this work due to their small concentration in the mixture with CLC. Both, azo NLCs 1005 and 1205 are mixtures of compounds of homologous series of 4-*n*-butyl-4'-*n*-alkoxyazobenzenes with structural formula

where R = CH_3, C_2H_5, ... C_5H_{11}. The composition of Merck's CLC hosts 1445 and BL061 which are used in this work are not known.

Large shifts in the baseline selective reflection wavelength from 470 to 670 nm are observed with increasing concentration. As indicated, the base CLC-mixture can accommodate large amounts of the azobenzene-based LC's, in this case greater than 20 wt%. This is unlike most dye-doped LC mixtures wherein the dye acts as an impurity and only small percentages are able to be incorporated before liquid crystallinity is lost. Here, two different azo-NLC's (1005 and 1205) were dissolved in two different commercially available CLC's. In all cases, as the concentration of the trans-azo-LC increased, the Bragg wavelength red-shifted indicating that the azo-LC material was acting to reduce the pitch of the material. Table 1 shows the series of mixtures examined in this work. Note that the limiting factor for concentration of azo LCs was the requirement to maintain the Brag wavelength of the mixtures in visible spectrum. Higher

than 25% shifts the reflection band into IR. The CLC-isotropic phase transition temperature is reduced by 10-15 degrees at such concentration of azo NLC.

Examining the dependence of the Bragg wavelength on UV exposure time for several of these compositions yields a rich variety of observed effects. Figure 2a shows the dependence of the Bragg wavelength on UV exposure time for several of these compositions. Several mixtures end up with a red-shifted notch while others show a final blue shift to the notch wavelength. The time scale of the process is driven by the power and wavelength of the irradiation source. For this figure, because the wavelength of exposure (395 nm) is outside the main absorption peak of the trans isomers and because of a low power density (~ 10 mW/cm^2) needed to compare all mixtures, the time constants are on the order of 100's seconds. Below, irradiation time scales on the order of nanoseconds are shown to induce similar effects. The change in the Bragg wavelength λ_B with exposure time is an indication that either the pitch and/or the average refractive index of the CLC material is changing. The high clearing temperature of these highly doped systems enables the mixture to retain its mesogenicity under prolonged exposure to UV and blue radiation. For most dye-doped systems wherein one uses radiation to enable the isothermal nematic-isotropic transition, mixtures which have clearing temperatures close to room temperature are the most effective. Here, by utilizing mixtures which have a high clearing temperature, large amounts of cis monomers can be achieved in the irradiated samples without causing the typical isothermal phase transition to occur. The temporal stability of the color obtained once irradiation is turned off is on the order of hours as shown in Figure 2b. Thus, any color can be 'dialed-in' by simply controlling the illumination time. The color change can be reversed by illumination of a green or red

laser wherein the reverse cis-trans reaction occurs, again on fast time scales as demonstrated later.

Figure 3 shows several visual representations of what happens when such mixtures are irradiated. The green outer part in Figure 3a is the original color of the CLC. A selective reflection wavelength in the blue (and thus a final blue shift) is obtained upon illumination with radiation of 409 nm wavelength and 3.2 mW power (68 mW/cm^2) power density. The green central spot is the restored color of the CLC that occurred upon exposure to a Ar+ laser beam of 488 nm of 0.37 mW power (108 mW/cm^2). The dynamics of such color shifts are shown in Figure 3b where the shaded areas mark the time intervals where the violet laser is exposing the original. The y-axes are the normalized reflection and transmission coefficient measured using the Ar^+ beam as a probe. Compared to Figure 2a, much faster time constants are realized and the effect of power density on both the relaxation and the restoration in this example is shown in Figure 3c. This speed can also be affected greatly by changing the illumination wavelength to 365nm as shown in Figure 3d. Because absorption and thus the production of cis isomers is so much more effective at this wavelength, faster switching speeds can also be realized. The insets show the color of 6 μm-thin films of the same sample, one after illumination of 532nm and the other after exposure to 365 nm radiation. The decrease of the response time with increasing power density of the UV radiation is demonstrated in Figure 4.

Figure 5 shows the photoinduced shift in the reflection spectra of CLC 1445 doped by 23 vol. % azo NLC 1205 [1205(23%)/1445] wherein the largest changes of Bragg wavelength is observed. Violet radiation of a LED matrix (λ = 395 nm, I = 10

mW/cm^2) tuned the position of the reflection band of this material from 625 nm to 1000 nm, an almost 400 nm shift in the peak wavelength. The effect of azo NLC concentration can be seen in Figure 5b where the magnitude of $\Delta\lambda_B$ is plotted for 3 μm-thick layers of 1005/1445 mixtures as a function of their exposure time to a violet laser beam (λ = 409 nm): the higher the concentration of azo NLC, the larger $\Delta\lambda_B$ and the sensitivity (steeper slope). At relatively large concentration values, $\Delta\lambda_B$ is a nonlinear function of azo NLC concentration which is expected given the proximity of the photoinduced isothermal phase transition region as indicated in Figure 5c. For all samples, the sign of the wavelength shift first is negative (blue shift) and then starts back towards the positive. Whether the final wavelength achieved is a net blue or red-shifted relative to the starting wavelength is highly dependent on the initial CLC mixture as shown in Table 1. For the azo NLC 1005 in CLC 1445, as concentration is increased, the final wavelength shift starts out at -1 nm reaches a maximum blue shift of -11 nm at 13% and then ends up at +134 nm at 25%. The same azo-LC material doped in BL061 starts at out with a -13 nm shift for 3 wt% increase to -46 nm at 11 wt%, and then comes back to a value of -31 nm for 25 wt%.

The mixtures we have studied are in the liquid crystalline phase at room temperature and are characterized with rather high clearing temperatures. The phase transition temperature from CLC to isotropic phase measured with 0.1°C accuracy for all mixtures is shown in Table 1. The effect of temperature on the Bragg wavelength is small compared to the effect of photoisomerization as it is seen in Figure 5d for two azo NLC doped CLC mixtures. The maximum thermally-induced shift of the Bragg wavelength is only $(\Delta\lambda_B)_T$ = 30 nm for the red-shifting mixture of azo NLC 1005 (25 wt.%) in CLC

1445 as opposed to $(\Delta\lambda_B)_{Ph}$ = 134 nm for phototuning. For the blue-shifting mixture of azo NLC 1005 (25 wt.%) in CLC BL061, we measured $(\Delta\lambda_B)_T$ = –3 nm, which is also nearly an order of magnitude smaller than the photoinduced shift equal to $(\Delta\lambda_B)_{Ph}$ = –31 nm. Practically no thermally-induced changes in the Bragg wavelength were registered for both materials up to 40°C as evident from figure 5d. Since phototunable properties of these materials were studied at room temperature using rather low power laser beams, we can conclude that the temperature of the materials does not change substantially and does not affect the photoinduced processes.

The wavelength of reflection is dictated by two parameters, the average index of refraction, n, and the pitch of the material, h. The average refractive index n of a CLC depends strongly on both the concentration of *cis* isomers and the strong influence of these isomers on the order parameter. The average refractive index n can be shown as $n = (n_{||} + n_{\perp})/2 = n_{\perp} + (n_{||} - n_{\perp})/2$. The optical anisotropy of the material $n_{||} - n_{\perp}$ decreases with decreasing order parameter which indicates that the effect of radiation *trans-cis* photoisomerization is to lower the overall average refractive index resulting in a finite blue shift of Bragg wavelength in all materials. The upper limit of the change of the average refractive index is set by phase transformation into an isotropic state:

$$\Delta n = \frac{n_{||} + n_{\perp}}{2} - \frac{n_{||} + 2n_{\perp}}{3} = \frac{n_{||} - n_{\perp}}{6} \qquad (1)$$

Although relatively small at $\Delta n \sim 0.03$ (for a typical value of the optical anisotropy of the material $n_{||} - n_{\perp} = 0.2$), this change can result in a change of the Bragg wavelength by as much as 20 nm as demonstrated. Thus blue shifts of this magnitude are

expected for highly doped samples wherein one lies close to the isothermal phase transition point.

The effect of changing the CLC pitch becomes prevalent, $n\Delta h > h\Delta n$, at longer exposure times due to, particularly, the slowness of director reorientation processes. The resulting shift in the Bragg wavelength, $\Delta\lambda_B = h\Delta n + n\Delta h$, becomes therefore red for mixtures with $\Delta h > 0$, or enhanced further in the blue for mixtures with $\Delta h < 0$. The magnitude of the CLC pitch h is determined by the concentration of the chiral molecules and is related to the helical twisting power of the molecular system. To a first approximation, any non-chiral molecule including both the trans and cis azo molecule will act as a dopant, reducing the helical twisting power of the system, thus red-shifting the wavelength as shown in Figure 1b. If the cis-molecule is more effective in "diluting" the chiral mesogenic order than the trans-molecule, a further red-shift is expected as a result of trans-cis photoisomerization. If the cis-molecule does not affect the internal structure as much (i.e. a shallower slope in Figure 1b), then one would expect a blue shift of the wavelength relative to the all-trans case. Any change in the pitch upon irradiation and thus formation of cis molecules other than that expected by the small change in refractive index indicates that the influence of the cis molecules as a dopant is thus different than the influence of the trans molecules. Data shown in Figure 6 confirms this behavior as the Bragg wavelength of CLC BL061 as a function of concentration of trans- and cis-isomers of azo NLC 1005 is shown. In order to control the quantity of the azo NLC for doping the CLC, a measured quantity of azo NLC 1005 was spread on a glass and was subjected to UV radiation (λ_{exp}= 365 nm, I=10 mW/cm^2) during 8 hours. The slope of the cis-isomer is shallower in this case indicating a weaker effect on the pitch.

Table 1 confirms that compared to the all-trans condition, this weaker influence on the pitch results in a net blue shift in wavelength.

The specific molecular details of the individual systems which dictate either a net blue shift (effective increase in the helical twisting power) or a red shift (effective decrease in the helical twisting power) is still unclear. Further experiments are underway to determine the large difference in behavior for the cis- and trans-molecules as doped into base CLC mixtures. Finite solubility places an upper limit for the change in the CLC pitch that can be obtained by increasing the dopant concentration in a CLC.

Photoinduced isomerization of azo molecules takes place within 10^{-9}s[22] as has been documented. One could expect therefore that CLC photosensitized by azo LC dopants should be responsive to short laser pulses due to the high energy density. A CLC 1005(7%)/BL061 mixture in a 6 μm-thick cell whose original Bragg wavelength was 535 nm first was exposed to UV radiation which shifted its reflection band towards violet wavelengths as shown previously in Figure 3d. Single shot laser pulses of nanosecond duration (532 nm) focused by a lens of 100 mm focal length proved capable of restoring (cis-trans isomerization) the green reflection state of the CLC. The sample was tested in different positions in the focal region of the lens for beam diameter values varying in the range 60-200 μm. The green spots seen over the area of Figure 7 were recorded by single laser pulses of nanosecond duration and 1-1.6 mJ energy due to the photoinduced shift of the CLC band gap from blue to green wavelengths. Although the detailed dynamics of the blue-to-green shift have not been studied yet, this transformation occurs on the order of microseconds. The spots, once formed, are stable on the order of an hour with the green spots relaxing back to the blue due to diffusive processes. Over extended periods

of time, the dark cis-trans relaxation will eventually convert the entire film to its energetically favorable green reflective state. The exposure energy density for the pulsed laser evaluated for the pulse energy value 1.6 mJ and beam diameter 0.6 mm results in 560 mJ/cm^2. This is close to the exposure energy density for CW radiation producing comparable shift in the Bragg wavelength (10 mW/cm^2 @ 40 s).

Figure 8 shows a set of lines recorded in photosensitized CLC cells by scanning it at the speed of 615 μm/s across a laser beam of nanosecond pulses at 10 Hz frequency. In these conditions, the travel distance of the cell from pulse to pulse is about 60 μm which is smaller than the radius of the beam on the sample (note again that the sample is out of the focus), hence the spots restored to their green reflection state overlap forming lines along the scan direction. The higher the pulse energy, the thicker the exposed lines.

Thus, single nanosecond pulses are capable of shifting the Bragg reflection band of the CLC from violet to green wavelengths. It will be very interesting in the future to study the dynamics of the restoration process in our future work and its dependence on pulse energy. Trans-cis photo-isomerization results in changing of the average refractive index both due to reduced order parameter as well as due to the difference of molecular polarizability of cis isomers from that of trans isomers.[23] The latter effect can affect the position of the Bragg reflection band of CLC within the pulse duration time.

3. Conclusion

In the present work, we have shown that doping CLC's with azo NLCs posessing large mesophase ranges is a promising approach to impart large, fast, and reversible

dynamic, photosensitive features in thin films formed using these mixtures. Large shifts in reflection wavelength with low laser power were demonstrated. These photosensitive features were demonstrated using both CW and nanosecond laser beams as was the ability to utilize these features to write, reversibly, information into the films. These photosensitive CLC materials will support opportunities for developing spectral as well as spatial filters with resolution and response times well beyond capabilities of electro-optical systems. Their design and manufacturing simplicity combined with low cost are important preconditions for their future applications and development of all-optical systems with customized properties. This work is enabled by the development of azo-based nematic liquid crystals which can be dissolved in CLCs in large concentrations without destroying the CLC structure enabling large photosensitivity.

4. Experimental

Two types of CLCs were used as hosts for azo NLC in the present study: BL061 and MDA-00-1445. These materials are available from Merck Ltd., exhibit Bragg reflection wavelengths of 467 and 468 nm and clearing temperatures of 86 and 94 C. The two types of azo NLC used for photosensitizing host CLCs are products of BEAM Engineering for Advanced Measurements Co. (BEAM Co.). The materials 1005 and 1205 two and three component compositions based on the series of 4-*n*-alkyl-4'-*n*-alkoxyazobenzenes

with R=CH_3 - 4-n-butyl-4'-methoxyzobenzene, R=C_2H_5 - 4-n-butyl-4'-ethoxyazobenzene, and R=C_5H_{11} - 4-n-butyl-4'-pentyloxyazobenzene. These compounds They are distinguished by a wide temperature range of the nematic phase including room temperature (12.5 N 49 I and 8 N 59 I, correspondingly) and birefringence values of 0.18 and 0.21. The optical anisotropy of the materials Δn is measured for at 633 nm wavelength.

Photosensitivity of these materials can be characterized by the so-called incubation energy E_{inc} which describes the initial stage of photoinduced nematic-isotropic phase transition.[24] Accumulation of cis isomers at this stage results in changing of the order parameter of the azo NLC without starting the critical process of phase transition. At this stage, the transmission of the material does not change even though the phase of a laser beam is changing according to the effect of order parameter on the refractive index of the material. The transmission of the material starts decreasing upon further accumulation of cis isomers due to generation of microdomains of isotropic phase. The energy required for completion of phase transition and obtaining homogeneous isotropic state E_{iso} is typically 2-3 times larger than the incubation energy. These parameters are equal to E_{inc} = 0.073 and E_{iso} = 0.13 J/cm^2 for azo NLC 1005, and E_{inc} = 0.39 and E_{iso} = 0.73 J/cm^2 for azo NLC 1205, correspondingly. The measurements were performed for 10-μm thick samples exposed to I_{inp}=6.2·10^{-3} W/cm^2 power density of a laser beam of 409 nm wavelength polarized parallel to the planar orientation of the azo NLCs.

Table 1 summarizes most material compositions tested in this work showing also the magnitude of the photoinduced shift in their Bragg wavelength, which is discussed further in this paper. In Table 1, L is the thickness of the material layer, λ_{exp} is the

wavelength of radiation inducing the shift of the Bragg wavelength, $\Delta\lambda_B$ is the magnitude of that shift.

---

[1] P. G. De Gennes, *Physics of Liquid Crystals,* Clarendon Press, Oxford, UK **1974.**

[2] L. M. Blinov, V.G. Chigrinov, *Electrooptic effects in liquid crystal materials*, Springer, New York, USA **1994**.

[3] G. D. Sharp, K. M. Johnson, D. Doroski, *Opt. Lett.* **1990**, *15*, 523.

[4] H. J. Masterson, G. D. Sharp, K. M. Johnson, *Opt. Lett.* **1989**, *14*, 1249.

[5] T. Ikeda, O. Tsutsumi, *Science* **1995**, *268*, 1873.

[6] T. Ikeda, *J. Mat. Chem.* **2003**, *13,* 2037.

[7] A. Urbas, J. Klosterman, V. Tondiglia, L. Natarajan, R. Sutherland, O. Tsutsumi, T. Ikeda, T. Bunning, *Advanced Materials* **2004,** *16*, 1453.

[8] S. Kubo, Z-Z. Gu, K. Takahashi, Y. Ohko, O. Sato, A. Fujishima, *J. Am. Chem. Soc.* **2002**, *124*, 10950.

[9] W. Haase, J. Adams, J. Wysocki, *Mol. Cryst. Liq. Cryst.* **1969**, *7*, 371.

[10] E. Sackmann, *J. Am. Chem Soc.* **1971**, *93*, 7088.

[11] N. V. Tabiryan, B. Ya. Zel'dovich, *Mol. Cryst. Liq. Cryst.* **1981**, *69*, 19.

[12] B. Ya. Zel'dovich, N. V. Tabiryan, *Sov. Phys. JETP* **1982**, *55*, 99.

[13] V. Vinogradov, A. Khizhniak, L. Kutulya, Yu. Reznikov, V. Reshetnyak, *Mol. Cryst. Liq. Cryst.* **1990**, *192*, 273.

[14] K. E. Asatryan, A. R. Mkrtchyan, Yu. A. Reznikov, N. V. Tabiryan, V. B. Vinogradov, *Opt. Spectrosc.* (USSR) **1990**, *69*, 495.

[15] S. Kurihara, T. Kanda, T. Nagase, T. Nonaka, *Appl. Phys. Lett.* **1998**, *73*, 2081.

[16] S. Kurihara, S. Nomiyama, T. Nonaka, *Chem. Mater.* **2000**, *12*, 9.

[17] N. Tamaoki, *Advanced Materials* **2001**, *13,* 1135.

[18] M. Moriyama, S. Song, H. Matsuda, N. Tamaoki, *J. Mater. Chem.* **2001**, *11*, 1003.

[19] S. V. Serak, E. O. Arikainen, H. F. Gleeson, V. A. Grozhik, J.-P. Guillou, N. A. Usova, *Liquid Crystals* **2002**, *29*, 19.

[20] A. Chanishvili, G. Chilaya, G. Petriashvili, D. Sikharulidze, *Mol. Cryst. Liq. Crys.* **2004**, *409*, 209.

[21] U. Hrozhyk, S. Serak, N. Tabiryan, T. J. Bunning, *Mol. Cryst. Liq. Cryst.* **2006**, *454*, 235. See also BEAM Co.'s catalog of room temperature azobenzene liquid crystal materials at www.beamco.com.

[22] Y. Yu, T. Ikeda, *J. Photochem. Photobiol. C: Photochemistry Reviews* **2004**, *5*, 247.

[23] N. Tabiryan, U. Hrozhyk, S. Serak, *Phys. Rev. Lett.* **2004**, *93*, 113901.

[24] N.V. Tabiryan, S.V. Serak, V.A. Grozhik, *J. Opt. Soc. Am. B*, **2003**, *20*, 538.

Table caption

Azo NLC-sensitized CLC compositions and photoinduced shift in their Bragg reflection band.

Table 1. Azo NLC-sensitized CLC compositions and photoinduced shift in their Bragg reflection band.

Azo NLC (BEAM)	CLC (Merck)	Azo NLC concentration in CLC [vol.%]	L [μm]	λ_B [nm]	λ_{exp} [nm]	$\Delta\lambda_B$ [nm]	T_{cl} [°C]
1205	1445	11	5	554	395	58	89
		23	5	623		377	84
			20	625		311	
1005	1445	0	3	470	409	0	94
		1		476		-1	93.8
		3		488		-3	92.8
		5		498		-6	91.7
		7		510		-10	90.9
		10		536		-17	89.6
		12		552		-16	89
		13		557		-11	88.4
		14		568		-8	87.5
		16		589		-6	86.7
		18		610		4	85.6
		20		632		43	85
		23		655		78	83.9
		25		676		134	83
1005	BL061	0	3	468	409	0	86
		3		501		-13	84.5
		7		535		-29	82
		9		552		-38	81
		11		570		-46	79
		25		683		-31	71

Figure captions

Figure 1. (a) Absorption spectra of representative azo-LC and b) Bragg reflection wavelength vs azo dopant concentration for mixture of 1005 in 1445 along with color inserts of 20-μm thick CLC cell fabricated from each material.

Figure 2. (a) Shift of the Bragg wavelength as a function of UV exposure time for several azo NLC/CLC compositions (λ_{exp} = 395 nm, I = 10 mW/cm^2): 1 – 1205(11%)/1445, L = 5 μm; 2 – 1205(23%)/1445, L = 5 μm; 3 – 1205(23%)/1445, L = 20 μm; 4 – 1005(11%)/1445, L = 30 μm; 5 – 1005(18%)/BL061, L = 20 μm. (b) Dynamics of Bragg reflection wavelength due to cis-isomer relaxation for UV pre-exposed material 1005(7%)/BL061. A CLC cell, 6-μm thick, was exposed to UV radiation (λ_{exp} = 365 nm, I = 10 mW/cm^2) for 1 minute and then the relaxation back to the original reflective wavelength was monitored. The time constant of Bragg reflection band restoration is approximately 28 hours.

Figure 3. (a) Photo of CLC cell 1005(7%)/BL061 that has been uniformly illuminated by a 409 nm laser beam causing a blue shift of the original color from green to blue. The center spot has been subsequently irradiated with an Ar+ laser at 488 causing the relaxation of this area back to the green. (b) Dynamics of both processes as monitored using the Ar+ laser at 488 nm. (c) The effect of power density on the time constant for both processes (d) The spectral shift of this material as a function of time for irradiation of 365 nm and 532 nm wavelength sources (10 mW/cm^2).

Figure 4. (a) Bragg reflection wavelength vs exposure time for the material 1005(18%)/1445 (λ_{exp} = 395 nm, I = 10 mW/cm^2): 1 – 1 mW/cm^2; 2 – 1.2 mW/cm^2; 3 - 1.9 mW/cm^2; 4 – 2.8 mW/cm^2; 5 – 5.9 mW/cm^2 ; 6 – 8.2 mW/cm^2, 7 – 11.2 mW/cm^2; 8 – 18.3 mW/cm^2. (b) Time constant as a function of power density.

Figure 5. (a) Photoinduced shift in the relative Bragg reflection band of 5 μm thick CLC 1205(23%)/1445 upon illumination by a violet LED (λ_{exp} = 395 nm, I = 10 mW/cm^2): (a) absorption spectrum. The corresponding exposure times are: 1 – 0 s; 2 – 30 s; 3 – 60 s; 4 – 90 s; 5 – 120 s; 6 – 180 s; 7 – 300 s. (b) Shift of the Bragg wavelength as a function of exposure time for different concentration of azo NLC 1005 in CLC 1445: 1 – 1 vol.%; 2 – 23 vol.%; 3 – 25 vol.%. The thickness of the material samples in these tests is 3 μm, and they are exposed to a violet laser beam (λ_{exp} = 409 nm). (c) Reflection band shift vs azo NLC concentration for two compositions: 1005/1445 (1) and 1005/BL061 (2). (λ_{exp} = 409 nm, I = 10 mW/cm^2, exposure time is 60 s). (d) Thermally induced shift of Bragg wavelength for red-shifting CLC composition 1005(25%)/1445 (1) and blue-shifting CLC composition 1005(25%)/BL061 (2).

Figure 6. Bragg reflection wavelength for the composition 1005/BL061 as a function of concentration of azo NLC 1005 in trans-form (1) and in cis-form (2) to the CLC BL061. The cis-form of azo LC 1005 was obtained by exposing the material to UV radiation (λ_{exp} = 365 nm) for 6-hours.

Figure 7: Examples of restoration of the green reflection wavelength by single laser pulses of nanosecond duration: (a) and (b) correspond to different focusing conditions.

Figure 8. (a) Photo of a CLC cell with a set of lines recorded in a L = 6 μm-thick layer of the CLC 1005(7%)/BL061 by scanning it at the speed of 615 μm/s across a laser beam of nanosecond pulses at 10 Hz frequency and λ = 532 nm wavelength. The beam is focused

by a lens of $F = 100$ mm focal length. Pulse energy: 55 μJ; distance between the lines: 0.5 mm; line thickness: 160 μm. (b) Photo taken under microscope.

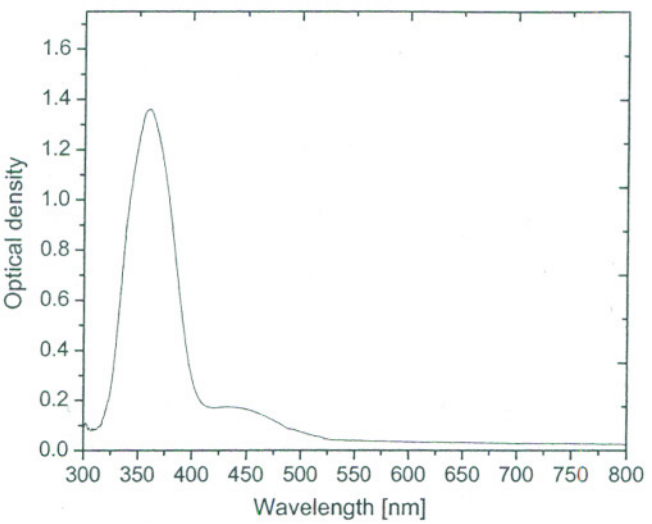
Optical density
1.6
1.4
1.2
1.0
0.8
0.6
0.4
0.2
0.0
300 350 400 450 500 550 600 650 700 750 800
Wavelength [nm]

Figure 1a

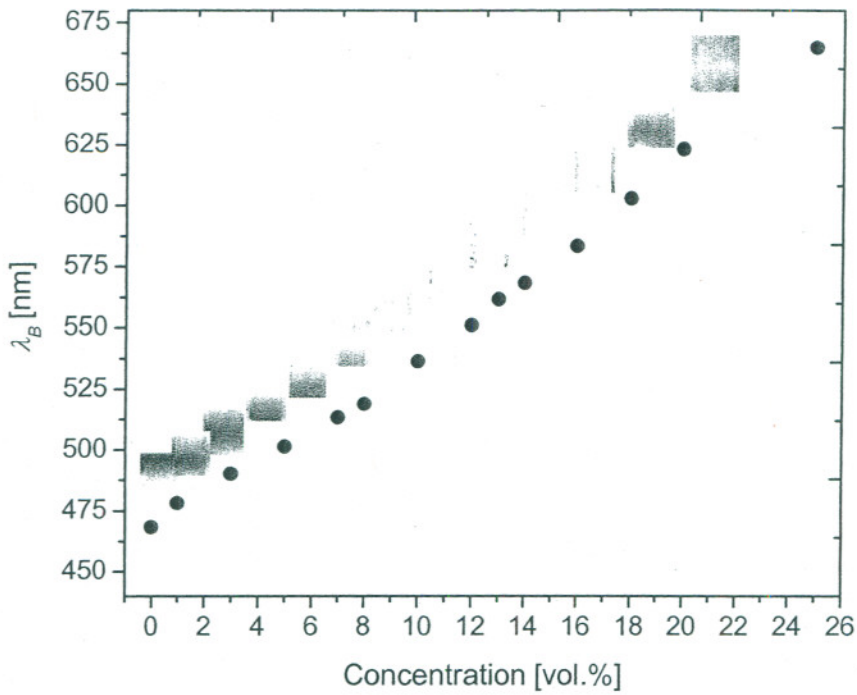
675
650
625
600
575
550
525
500
475
450
λ_B [nm]
0
2
4
6
8
10
12
14
16
18
20
22
24
26
Concentration [vol.%]

Figure 1b

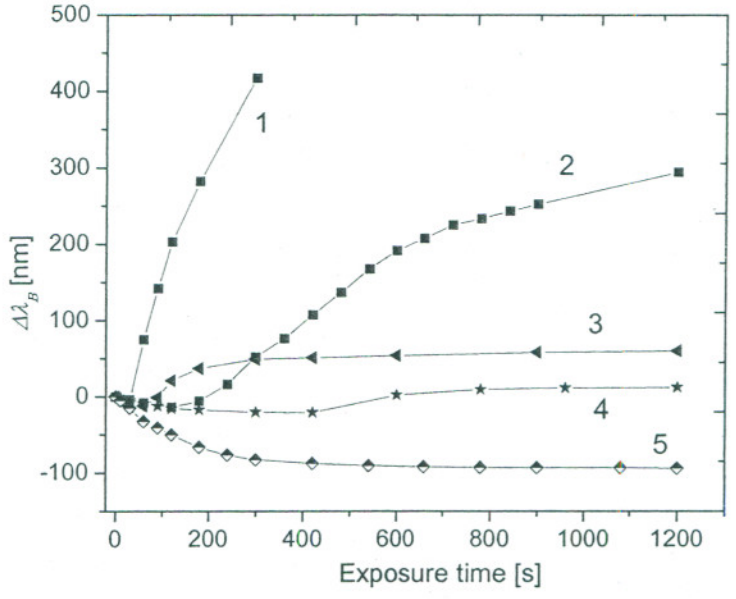
500
400
300
200
100
0
-100
$\Delta\lambda_B$ [nm]
0
200
400
600
800
1000
1200
Exposure time [s]
1
2
3
4
5

Figure 2a

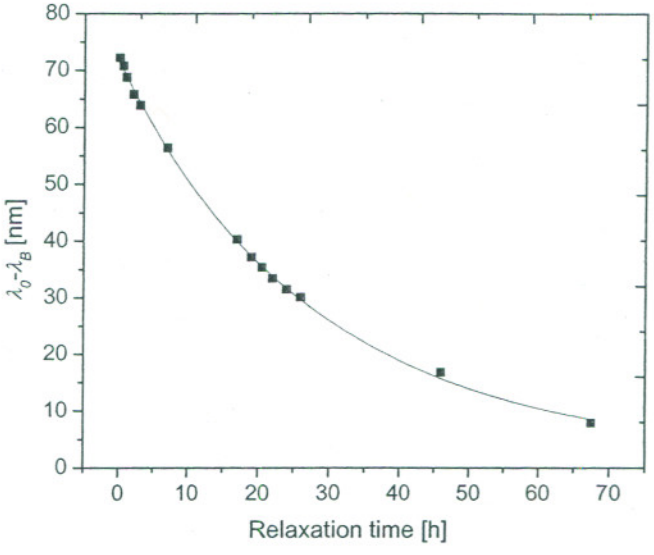
80
70
60
50
40
30
20
10
0
λ_0-λ_B [nm]
0
10
20
30
40
50
60
70
Relaxation time [h]

Figure 2b

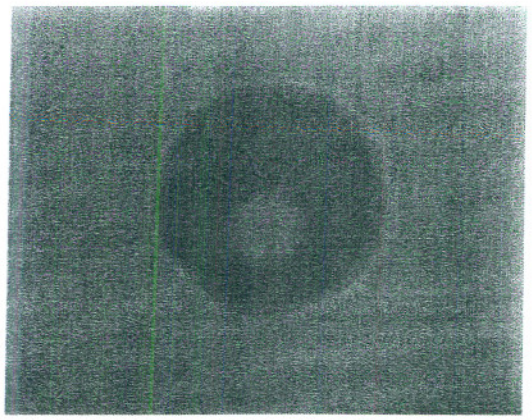

Figure 3a. Photo of CLC cell 1005(7%)/BL061

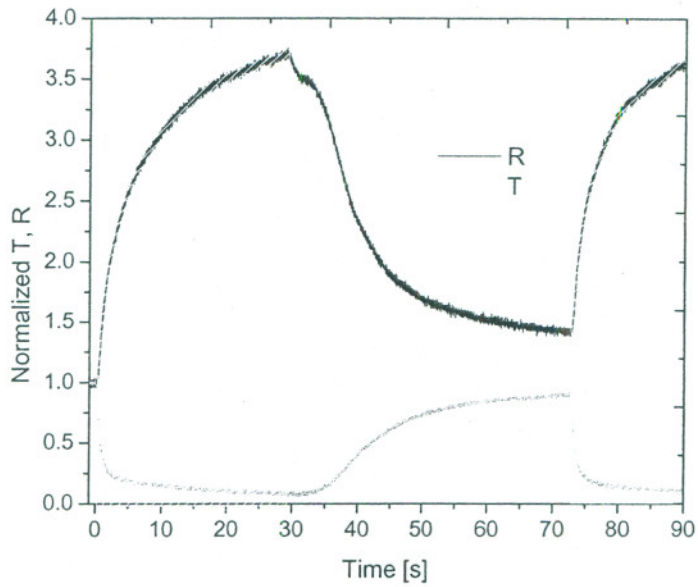
4.0
3.5
3.0
2.5
2.0
1.5
1.0
0.5
0.0
Normalized T, R
R
T
0
10
20
30
40
50
60
70
80
90
Time [s]

Figure 3b

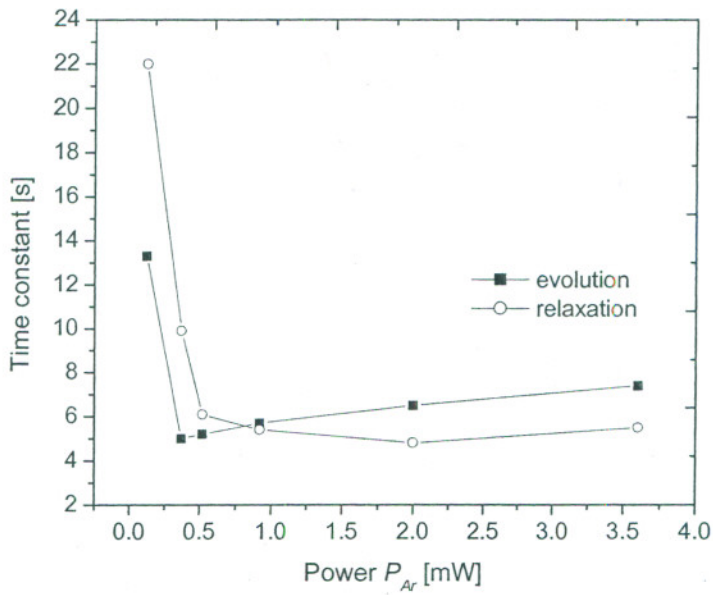
Time constant [s]
Power P_{Ar} [mW]
evolution
relaxation
24
22
20
18
16
14
12
10
8
6
4
2
0.0
0.5
1.0
1.5
2.0
2.5
3.0
3.5
4.0

Figure 3c

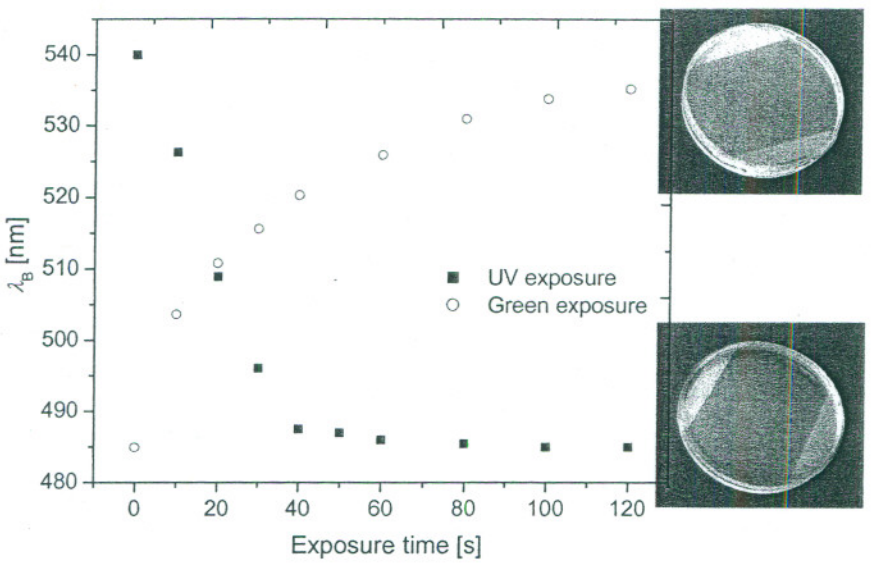
540
530
520
510
500
490
480
λ_B [nm]
0
20
40
60
80
100
120
Exposure time [s]
UV exposure
Green exposure

Figure 3d

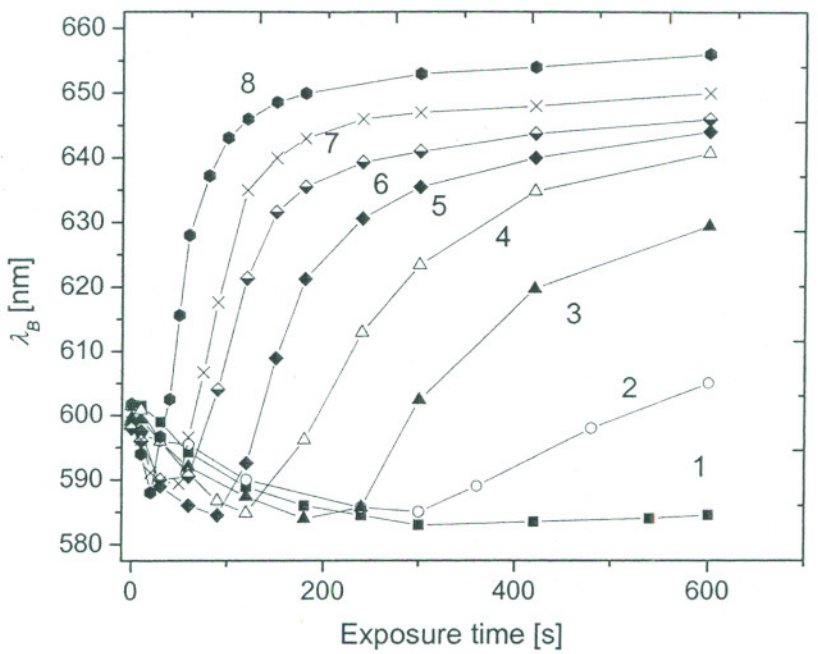
660
650
640
630
620
610
600
590
580
λ_B [nm]
0
200
400
600
Exposure time [s]
8
7
6
5
4
3
2
1

Figure 4a

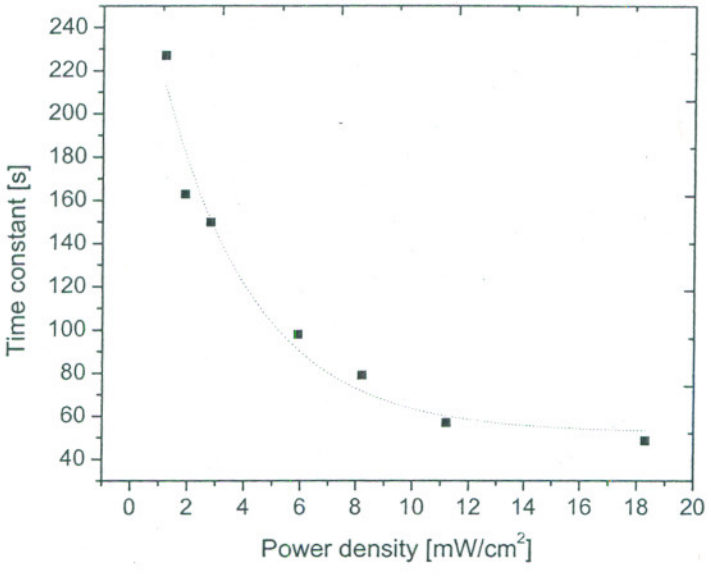
Time constant [s]
240
220
200
180
160
140
120
100
80
60
40
0
2
4
6
8
10
12
14
16
18
20
Power density [mW/cm^2]

Figure 4b

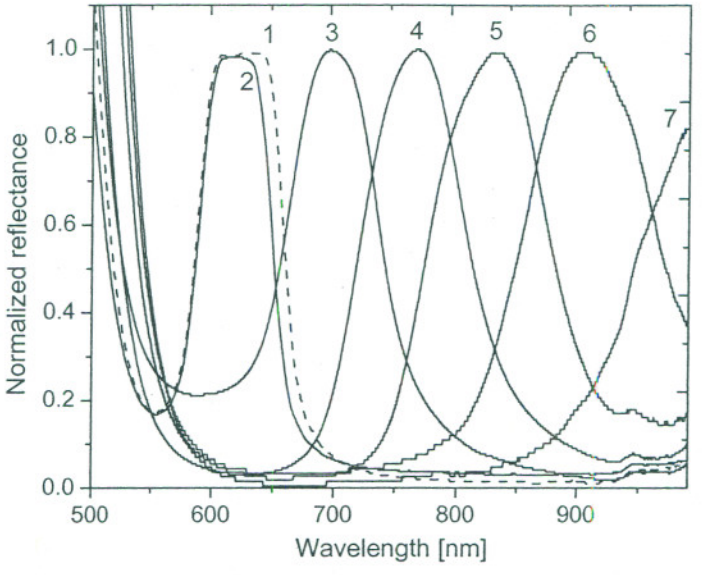
Normalized reflectance
1.0
0.8
0.6
0.4
0.2
0.0
500
600
700
800
900
Wavelength [nm]
1
2
3
4
5
6
7

Figure 5a

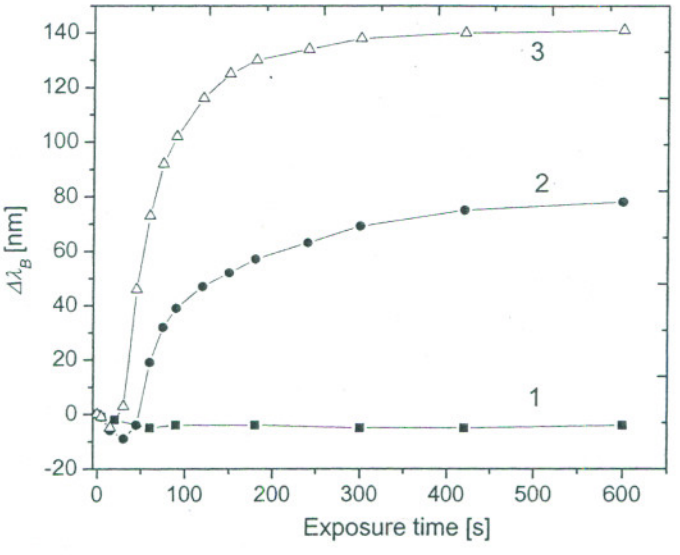
140
120
100
80
60
40
20
0
-20
$\Delta\lambda_B$ [nm]
0
100
200
300
400
500
600
Exposure time [s]
1
2
3

Figure 5b

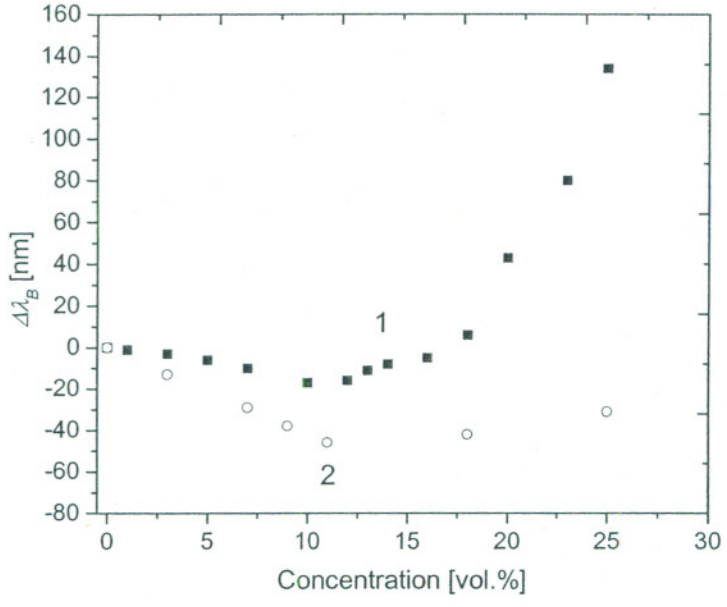
160
140
120
100
80
60
40
20
0
-20
-40
-60
-80
$\Delta\lambda_B$ [nm]
1
2
0
5
10
15
20
25
30
Concentration [vol.%]

Figure 5c

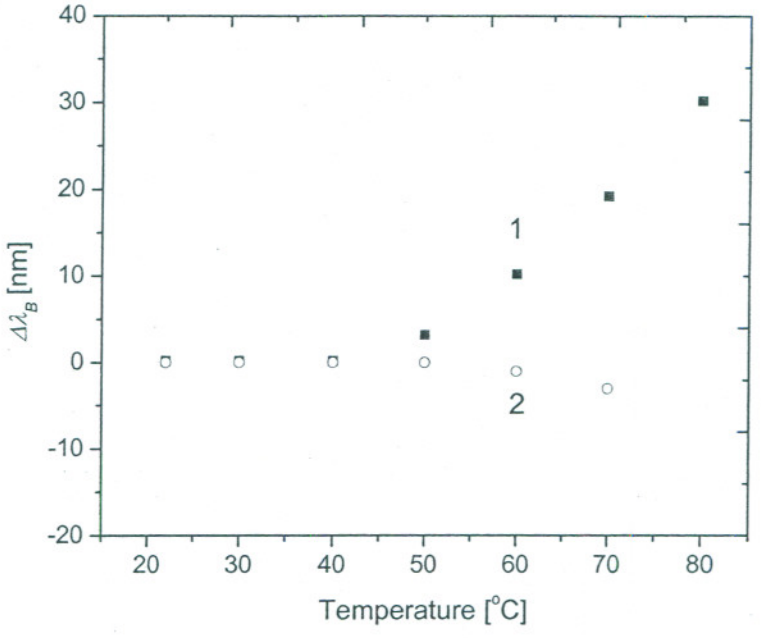
40
30
20
10
0
-10
-20
$\Delta\lambda_B$ [nm]
1
2
20
30
40
50
60
70
80
Temperature [°C]

Figure 5d

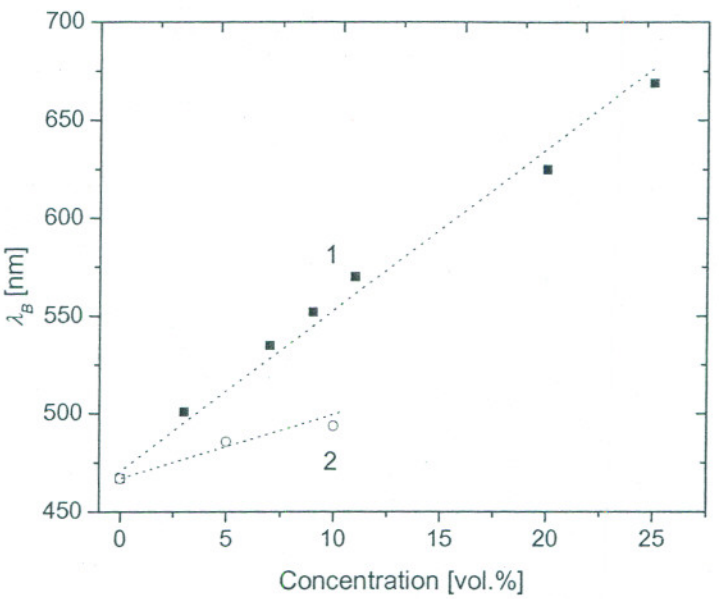
700
650
600
550
500
450
λ_B [nm]
1
2
0
5
10
15
20
25
Concentration [vol.%]

Figure 6

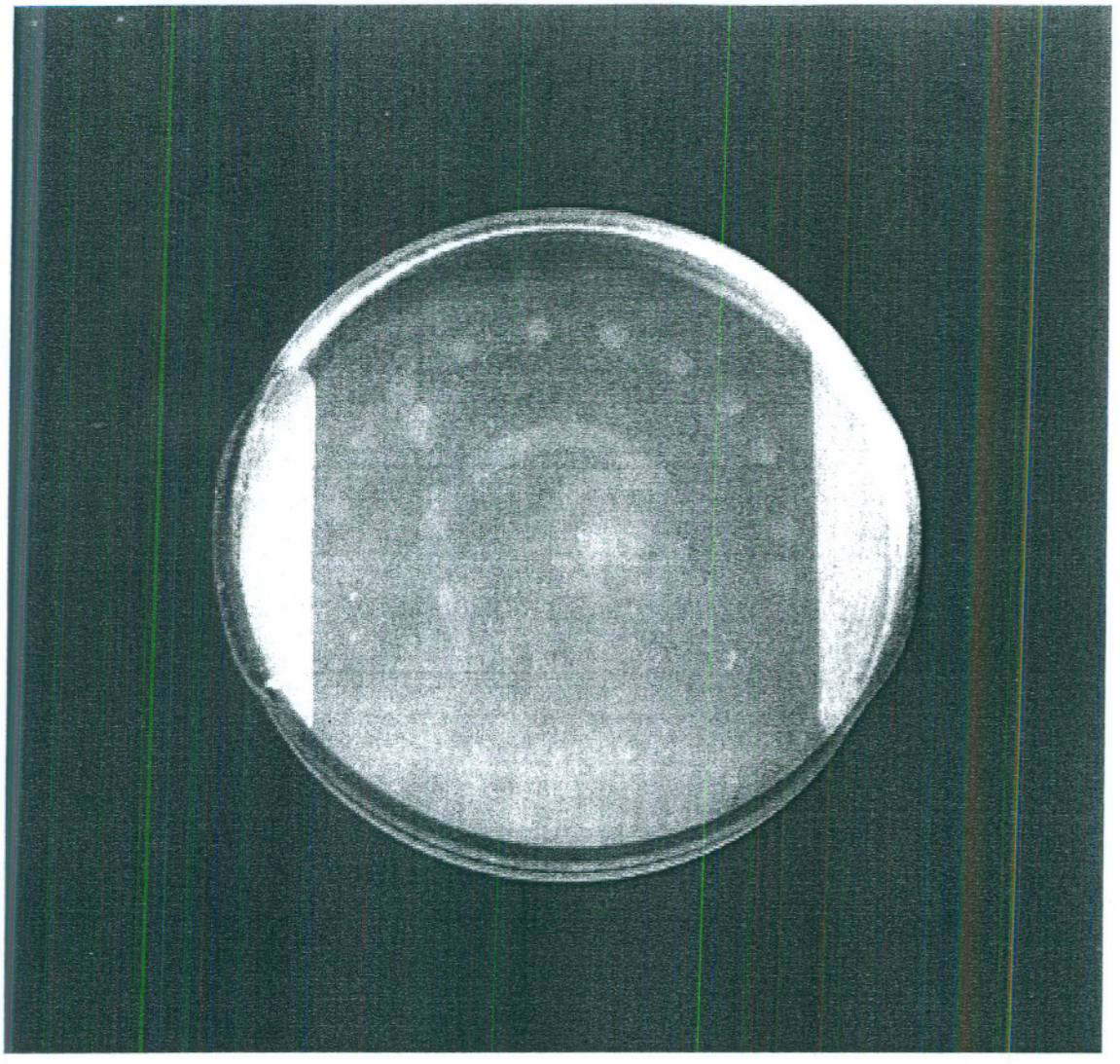

Figure 7a. Example of restoration of the green reflection wavelength by a single laser pulse of nanosecond duration, focus condition 1

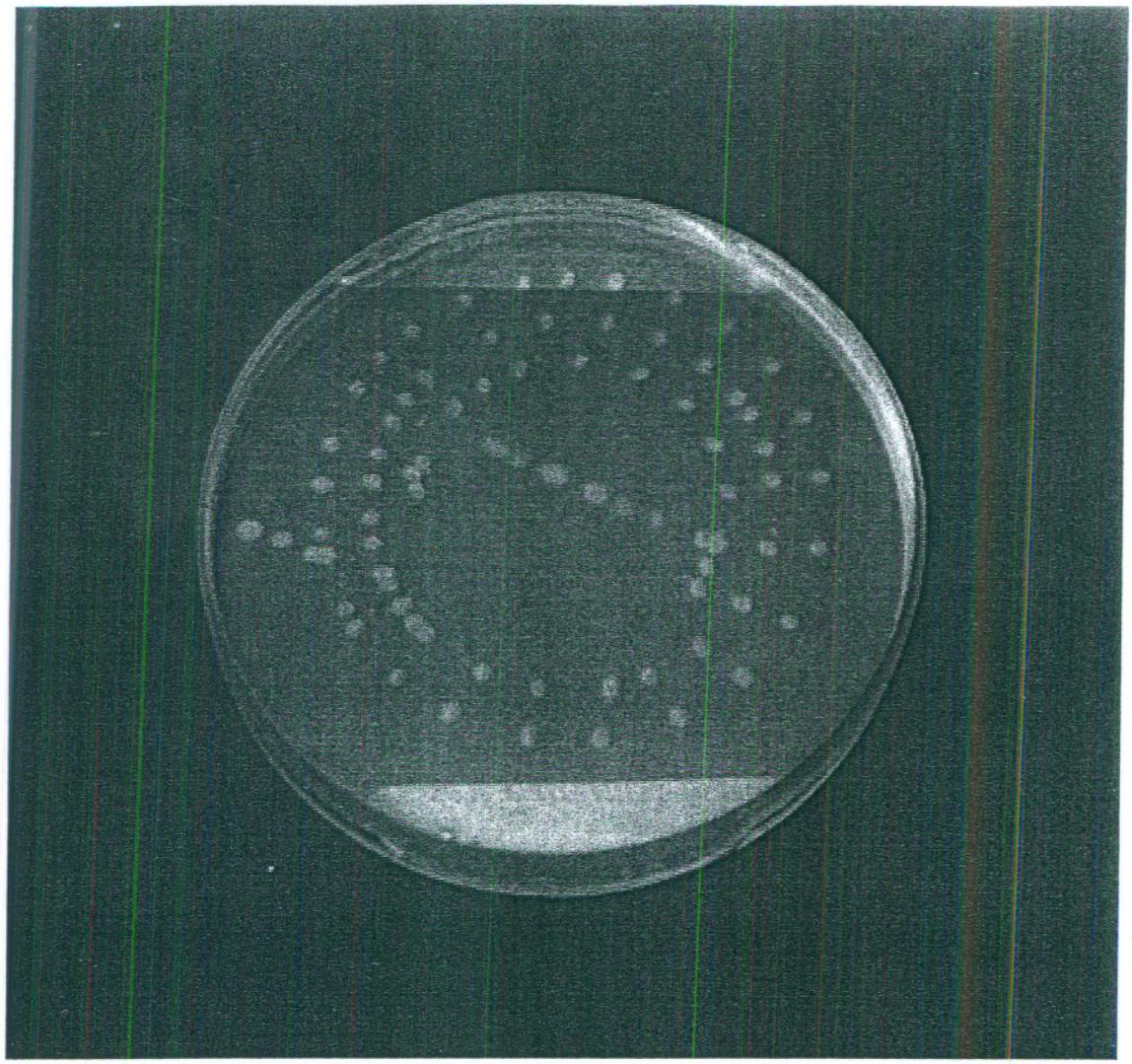

Figure 7b. Example of restoration of the green reflection wavelength by a single laser pulse of nanosecond duration, focus condition 2

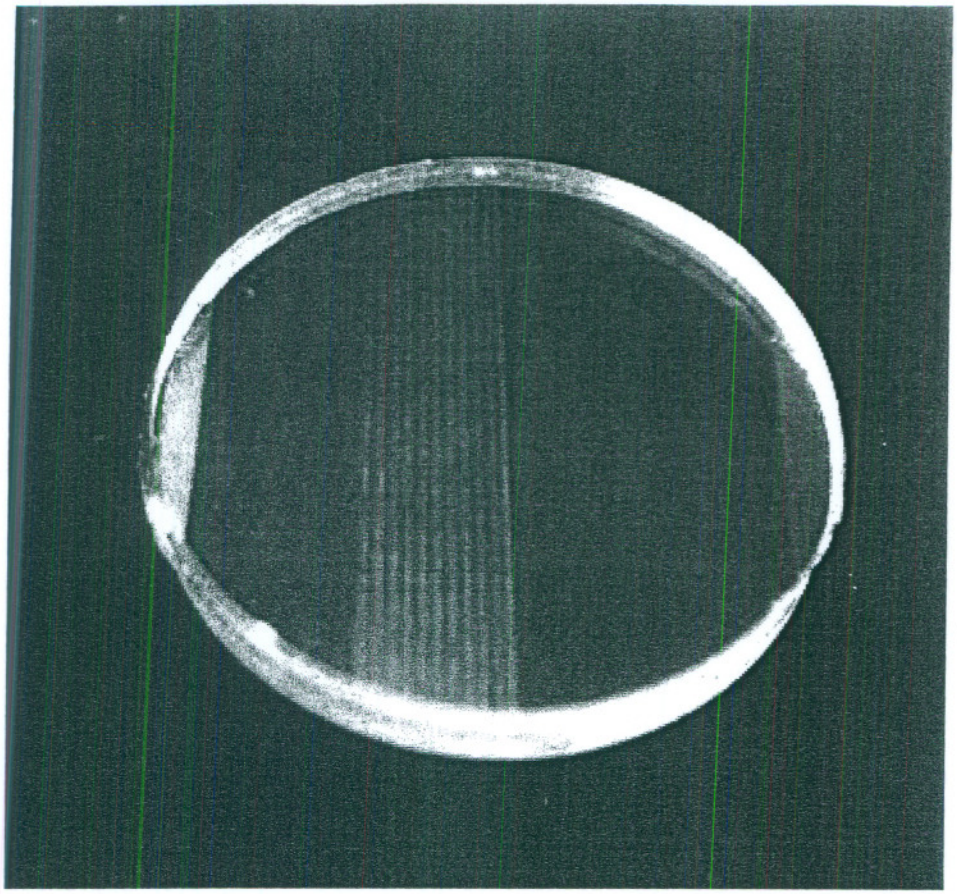

Figure 8a. Photo of a CLC cell with a set of lines recorded in a L = 6 um-thick layer of the CLC 1005(7%)/BL061 by scanning at a speed of 615 um/s across a laser beam of nanosecond pulses

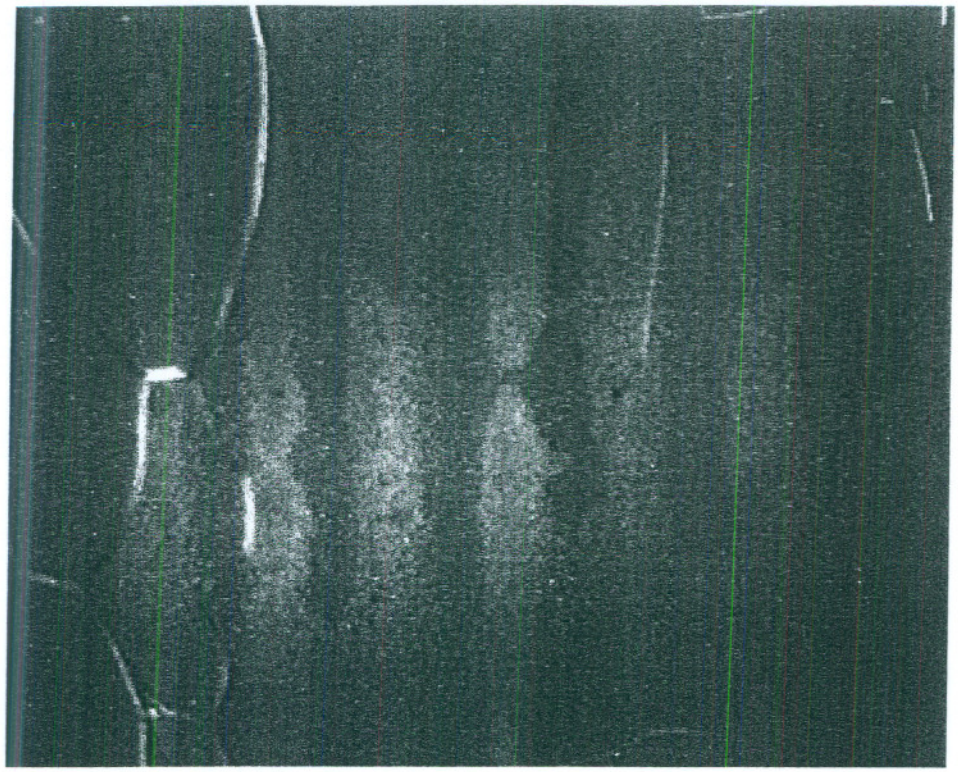

Figure 8b. Photo taken under